Available online at www.sciencedirect.com
ScienceDirect
Journal of Power Sources 173 (2007) 510–517
JOURNAL OF POWER SOURCES
www.elsevier.com/locate/jpowsour

Anodic behavior of Al current collector in 1-alkyl-3-methylimidazolium bis[(trifluoromethyl)sulfonyl] amide ionic liquid electrolytes

Chengxin Peng [a], Li Yang [a,*], Zhengxi Zhang [a], Kazuhiro Tachibana [b], Yong Yang [c]

[a] *School of Chemistry and Chemical Technology, Shanghai Jiao tong University, Shanghai 200240, China*
[b] *Department of Chemistry and Chemical Engineering, Yamagata University, Yamagata 992-8510, Japan*
[c] *State key lab for Physical Chemistry of solid surface, Xiamen University, Xiamen 361005, China*

Received 13 January 2007; received in revised form 25 April 2007; accepted 3 May 2007
Available online 7 May 2007

Abstract

The anodic behaviors of aluminum current collector for lithium ion batteries were investigated in a series of 1-alkyl-3-methylimidazolium bis[(trifluoromethyl)sulfonyl] amide room temperature ionic liquids (RTILs) and EC + DMC electrolytes. It was found that the aluminum corrosion, which occurred in EC + DMC electrolytes containing LiTFSI, was not observed in the RTIL electrolytes. Further research showed that a passive film with amide compounds as main components formed firmly on aluminum surface during the anodic polarization in the RTIL electrolytes, which inhabited the aluminum corrosion. In addition, the additives generally used in the batteries, such as ethylene carbonate, ethylene sulfite and vinyl carbonate, as well as temperature did not obviously affect the aluminum passive film, the oxidation of the RTILs increased at the elevated temperature, which only resulted in the corrosion potential of aluminum in the RTIL electrolytes shifted to more negative potential, a passive film still firmly formed on the aluminum surface to surpassed the further oxidation of the aluminum current collector. Those results lead to a potential for the practical use of LiTFSI salt in the room temperature ionic liquid electrolytes for lithium ion batteries.

Keywords: Lithium ion battery; Al current collector; Corrosion; Ionic liquid; Additive

1. Introduction

Advanced energy batteries are now more required for energy storage and electric vehicle (EV) applications [1]. Therefore, novel electrode materials and electrolytes are expected to be found to match these demands. So far, many improvements about high-density positive materials were published [2], it brought about much progress on the corresponding electrolytes and other battery materials research. Lithium hexafluorophosphate ($LiPF_6$) is the most commonly used as lithium salt in conventional electrolytes for secondary commercial lithium ion batteries, because its electrolyte shows high ion conductivity and good electrochemical stability. However, $LiPF_6$ suffers from both thermal and hydrolytic instability, which lead to poor cycling performance and the unsafety for lithium ion batteries [3]. To solve the above problem, a new candidate of lithium salt, bis[(trifluoromethyl)sulfonyl] amide [$LiN(CF_3SO_2)_2$, LiTFSI], with greater thermal and hydrolytic stability, good conductivity and high electrochemical stability were investigated. Unfortunately, the practical use of LiTFSI in carbonate-based electrolytes hardy realized due to severe corrosion of aluminum (Al) current collectors above about 3.5 V versus Li^+/Li [3–10]. Behl and Plichta [11] reported that the addition of $LiBF_4$ to 1 M LiTFSI/EC-PC-DMC significantly suppress the aluminum corrosion during potentiostatic polarization process. A similar beneficial effect of added $LiBF_4$ and $LiPF_6$ on the stability of aluminum in LiTFSI electrolytes had also been described [4,5,7,12,13]. However, the volatile and flammable organic solvent involved in the conventional electrolytes may result in the unsafety of lithium ion battery, especially at higher temperature.

Recently, room temperature ionic liquids (RTILs), showing excellent properties of good electrochemical, non-flammable and thermal stability [14–19], were investigated as new promising electrolytes for lithium ion batteries. Among these RTILs, the liquids based on $TFSI^-$ were presently regarded as the most suitable electrolytes for lithium ion batteries [20] and

* Corresponding author. Tel.: +86 21 54748917; fax: +86 21 54741297.
E-mail address: liyangce@sjtu.edu.cn (L. Yang).

0378-7753/$ – see front matter © 2007 Elsevier B.V. All rights reserved.
doi:10.1016/j.jpowsour.2007.05.006

also it has better solubility for LiTFSI salt. Up to date, few works had been carried out to investigate the electrochemical behavior of aluminum current collector in RTILs based on imidazolium cations. One research group [21,22] ever showed that aluminum passivates easily in 1-ethyl-3-methylimidazolium bis[(trifluoromethyl)sulfonyl] amide (EMI-TFSI) and 1-ethyl-3-methylimidazolium bis[(perfluoroethyl)sulfonyl] amide (EMI-BETI). However, there were no reports for the anodic behavior of the Al current collector in the RTILs based on different cations. Moreover, in practical use of lithium ion battery, some additives were chosen to add into those RTILs to form a solid electrolyte interface (SEI) on the negative electrode, which inhibited the electrolytes decomposition on lithium or lithiated carbon surface [23,24] because those RTILs lack electrochemical stability up to the reduction potential of lithium or lithium carbon [20,23].

In this work, the anodic behaviors of Al foil electrode in a series of 1-alkyl-3-methylimidazolium bis[(trifluoromethyl) sulfonyl] amide ionic liquids containing LiTFSI were studied. Besides, the influences of additives and temperature on the anodic behaviors of aluminum current collector were also investigated using cyclic voltammetry (CV), scanning electron microscopy (SEM), Fourier transformed infrared spectroscopy (FT-IR) and energy dispersive X-ray spectroscopy (EDX) measurements in order to find more suitable electrolytes with better compatibility between RTILs and the aluminum current collector for lithium ion batteries and other electrochemical devices.

2. Experimental

LiTFSI salt (99.9%, Morita) was dried under a vacuum at 120 °C for 24 h prior to use. Room temperature ionic liquids based on anion $TFSI^-$, 1-ethyl-3-methylimidazolium bis[(trifluoromethyl)sulfonyl] amide (EMI-TFSI), 1-propyl-3-methylimidazolium bis[(trifluoromethyl)sulfonyl] amide (PMI-TFSI) and 1-butyl-3-methylimidazolium bis[(trifluoromethyl) sulfonyl] amide (BMI-TFSI) were prepared in our laboratory according to usual synthesis [25] and treated with molecular sieves (4 Å) for 2 days to dehydrating and had the water content in them were less than 20 ppm determined by Karl Fisher titration method before making solutions (Fig. 1 shows their chemical structures). LiTFSI salt was dissolved in EMI-TFSI, PMI-TFSI, BMI-TFSI and EC + DMC (1:1 in vol.) to make 1 mol dm^{-3} (M) solutions. Ethylene carbonate (EC) (99%), ethylene sulfite (ES) (98%, Aldrich), and vinyl carbonate (VC) (98%, Acros) was used as additives into the RTILs, respectively.

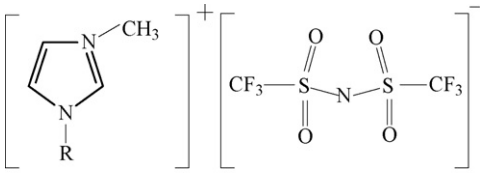

Where in R= CH_2CH_3 EMI-TFSI
= $CH_2CH_2CH_3$ PMI-TFSI
= $CH_2CH_2CH_2CH_3$ BMI-TFSI

Fig. 1. Chemical structures of RTILs.

The anodic polarization behaviors of aluminum electrode were investigated using CHI 604B electrochemical work-station (CH Instruments, U.S.A.). A standard cell (inner volume: 10 cm^3) with three electrodes was applied to this experiment. Aluminum foil was dipped in 1.0 mol dm^{-3} NaOH solution for 180 s and then rinsed for 20 s with deionized water to eliminate the oxidation on its surface. The degreased aluminum foil was neutralized with 0.65 mol dm^{-3} HNO_3 for 30 s and also rinsed with deionized water for 60 s, respectively. After drying under vacuum, the pretreated Al electrode (geometric surface area: 1.0 cm^2) was used as working electrode, reference and counter electrode were both lithium (Li) metal. The cyclic voltammetry of aluminum in the above electrolytes was performed for three times which swept from natural potential to 5.5 V versus Li^+/Li for the first anodic scan and return to 1.5 V versus Li^+/Li with a potential scan rate of 10.0 mV s^{-1}. The electrolytes preparation process and electrochemical measurement were conducted in UNiLab glove box filled with argon (Ar) atmosphere at ambient temperature, unless otherwise specified in the text.

The aluminum electrode after the anodic polarization was well rinsed by dimethyl carbonate solvent and then dried at room temperature under vacuum for 24 h. This prepared aluminum electrode was set on a sample holder of scanning electron microscopy (SEM) (FEI Sirion 200, FEI, U.S.A.) camber to observe the surface morphology and examine the elements by energy dispersive X-ray spectroscopy (EDX) (Oxford Inca, Oxford, U.K.).

Fourier transformed infrared spectroscopy (FT-IR) (Paragon 1000, Perkin-Elmer, U.S.A.) measurement was also applied to analyze the corrosion products on aluminum surface after the anodic polarization. The aluminum samples preparation was similar to that in the SEM experiments. The FT-IR measurements were conducted on an attenuated total reflection (ATR) accessory using the reflectance technique (4000–450 cm^{-1}). The single beam reference FT-IR spectrum was first taken from an open area of mirror polished aluminum surface. Samples information of FT-IR spectra acquired from the area covered by passive film then ratioed to the reference spectrum, and converted into absorbance. All the spectra were acquired at 4 cm^{-1} resolution, with a total of 512 scans co-added. The samples were enclosed in an Ar-filled device during the measurement to avoid air exposure.

3. Results and discussion

3.1. The anodic behavior of Al electrode in neat RTILs

The electrochemical windows of EC + DMC containing 1 M LiTFSI and RTILs were tested by cyclic voltammetry on platinum electrode with a sweep rate of 10.0 mV s^{-1}, using Li foil as a counter and reference electrode. As shown in Fig. 2, the reduction potential of RTILs occurred at around 1.5 V versus Li^+/Li, which was less negative than that of 1 M LiTFSI/EC + DMC at 0.5 V versus Li^+/Li, while the oxidation potential of RTILs is around 6.0 V versus Li^+/Li, slightly positive than that of 1 M LiTFSI/EC + DMC at 5.7 V versus Li^+/Li.

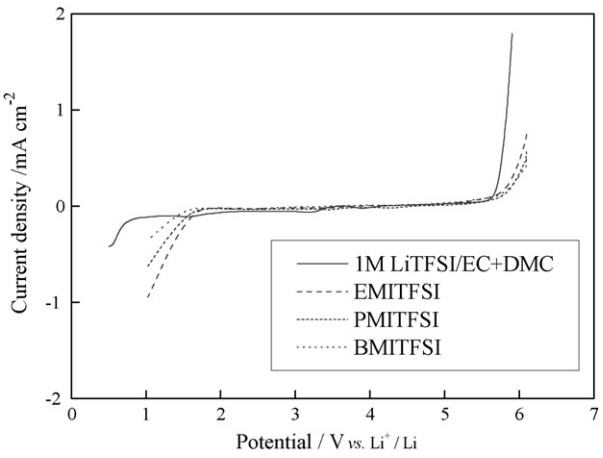

Fig. 2. Linear sweep voltammetry on platinum at EC + DMC containing 1 M LiTFSI and RTILs (sweep rate: 10.0 mV s^{-1}).

The electrochemical behavior of the pretreated Al foil electrode in electrolytes was investigated by cyclic voltammetry. The anodic potential range has been limited from 1.5 to 5.5 V versus Li^+/Li to ensure that no electrolytes degradation occurred. As shown in Fig. 2, almost no current was observed obviously in the potential range 1.5–5.5 V versus Li^+/Li from the above four electrolytes.

Fig. 3(a) showed typical CVs of the Al foil electrode in EC + DMC containing 1 M LiTFSI. To compare with the anodic behavior of Al foil in the RTIL electrolytes, EC + DMC solutions were chosen as the organic electrolytes for the cyclic voltammetry measurements. As previously reported [8], corrosion occurred on the Al surface after the potential cycling in carbonate-based electrolytes. In this electrolyte, it was found that the anodic current increased abruptly at about 5.0 V versus Li^+/Li (hereafter called it as pitting potential, E_p) during the first anodic scan, which implied that the dissolution of aluminum occurred on the Al anode surface. However, a higher anodic current during the reverse potential scan showed that the process accompanied by a corrosion step on the Al foil electrode surface. In the second cycle, corrosion started at about 3.7 V versus Li^+/Li, which is lower than that of the first cycle by about 1.3 V. This fall of corrosion potential was ascribed to the loss of the less protective surface film formed in the first cycle, which induced the aluminum foil to be more easily corroded in the next cycles. Furthermore, the current peak in second cycle was almost 20 mA cm^{-2} at 5.5 V versus Li^+/Li, which is higher than that of the first cycle, showing the aluminum corrosion became more and more serious after the breakdown of protective film.

The voltammetric responses of the Al foil electrode in RTILs electrolytes were shown in Fig. 3(b)–(d), a weaker anodic current was observed at about 3.0 V versus Li^+/Li at the first scan, and it rapidly decreased during the reverse potential sweeps. Besides, the anodic current was less than 0.02 mA cm^{-2}, which was much smaller than that in EC + DMC electrolyte. During the followed cycles, the corrosion potential rose higher than 5.0 V versus Li^+/Li. The shape of the cyclic voltammograms of the Al foil electrode in RTILs electrolytes look like each other. This suggests that the anodic polarization processes on the Al electrode are essentially the same in these RTILs. From the results, it could be seen that Al electrode is completely passivated during the first scan in the RTIL electrolytes. That is, Al is stable anodically in the RTIL electrolytes due to the presence of a pas-

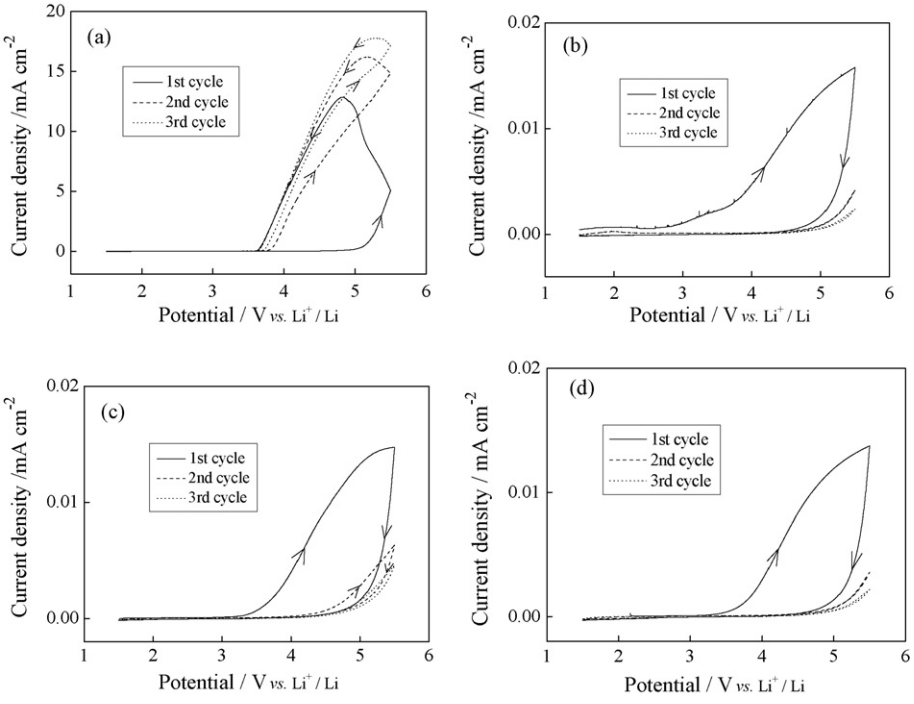

Fig. 3. Cyclic voltammograms for Al foil electrode in 1 M LiTFSI/EC + DMC (a); 1 M LiTFSI/EMI-TFSI (b); 1 M LiTFSI/PMI-TFSI (c); 1 M LiTFSI/BMI-TFSI (d) (sweep rate: 10.0 mV s^{-1}).

sive surface film at potentials above 5.0 V versus Li^+/Li. This behavior is favorable for the current collector of rechargeable lithium batteries because the aluminum corrosion, which easily occurred in carbonate-based electrolytes, can be inhibited by the RTILs. Furthermore, the passivation film formed on the surface during the anode polarization may be enhanced to resist more anodic potential. Collectively, the current response was different between Al foil electrode in EC + DMC and RTILs containing 1 M LiTFSI, which contributed to the different solvent in electrolytes. On the other hand, although the features of CV were similar among these RTILs containing 1 M LiTFSI showed that the similar passivation processes were performed on the Al electrode, there was also a slightly different current response of the Al foil among the three RTILs containing 1 M LiTFSI. In the first cycle, the E_p of the Al foil electrode in 1 M LiTFSI/EMI-TFSI is 2.8 V versus Li^+/Li, which was negative than those in 1 M LiTFSI/PMI-TFSI at 3.2 V versus Li^+/Li and 1 M LiTFSI/BMI-TFSI at 3.5 V versus Li^+/Li. It was hypothesized that the different structures of the RTIL affect the formation of passive film on the Al foil electrode during the anodic polarization. From those current responses of the RTILs, the change of E_p may be related to the change of alkyl chain length of the RTILs. With the length of the alkyl in the cation increasing from EMI-TFSI, PMI-TFSI to BMI-TFSI, the E_p of Al electrode in the RTILs shifted to more and more positive potential, which do benefit for the aluminum current collector of rechargeable lithium batteries.

Fig. 4 showed the SEM images for the Al foil surface after the potential sweep to 5.5 V for three times in EC + DMC and the RTILs containing 1 M LiTFSI. The potential cycling in the 1 M LiTFSI/EC + DMC electrolyte led to significant change in the surface imagine from the original one. As shown in the Fig. 4(a), corrosion pits of 5–20 μm size were observed on the Al foil surface, indicating that the destruction of the passivation film on the Al electrode surface took place in EC + DMC electrolytes, which induced to the increase of anodic current in the course of consecutive potential sweeps. However, the surface features after the same potential cycling in the RTILs in Fig. 4(b)–(d) showed that almost no corrosion was found on the surface except that some insoluble solid product cluster dotted on the Al surface compared to the fresh aluminum in Fig. 4(e), indicating that the Al electrodes were stable in those electrolytes. Presumably those clusters are the precipitates building up the passive layer deposited on the Al electrode which was produced by reacting aluminum and electrolyte and/or electrolyte decomposition at high potential. The SEM images confirmed that the

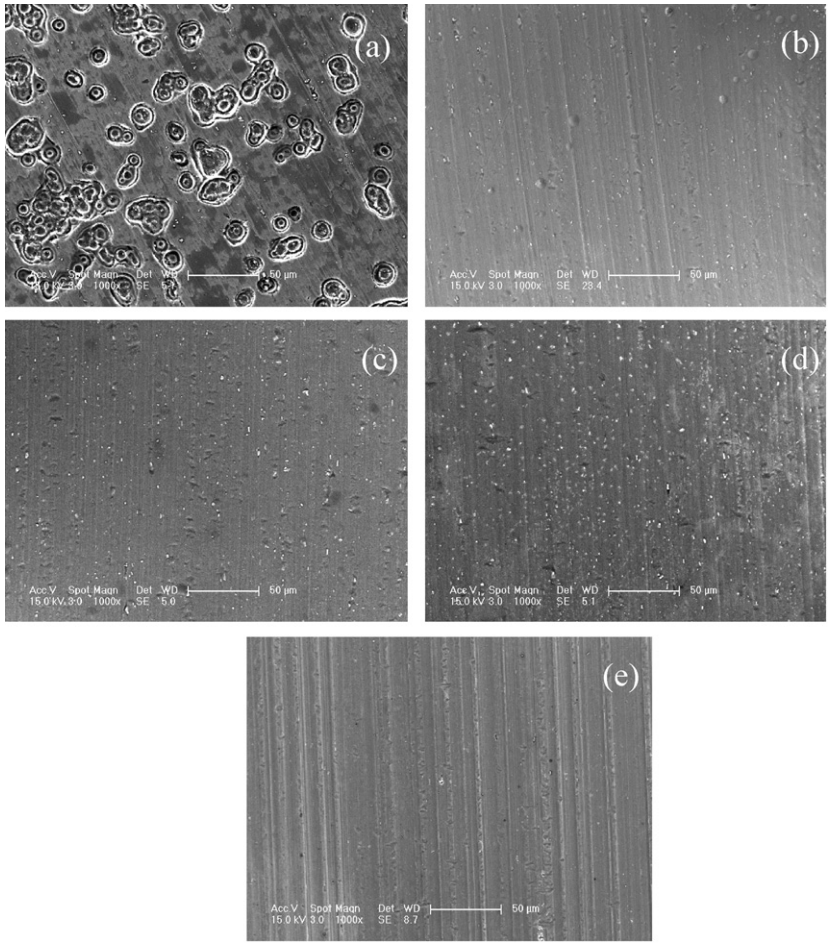

Fig. 4. SEM images of Al surface after the potential cycling in 1 M LiTFSI/EC + DMC (a); 1 M LiTFSI/EMI-TFSI (b); 1 M LiTFSI/PMI-TFSI (c); 1 M LiTFSI/BMI-TFSI (d); fresh aluminum foil (e).

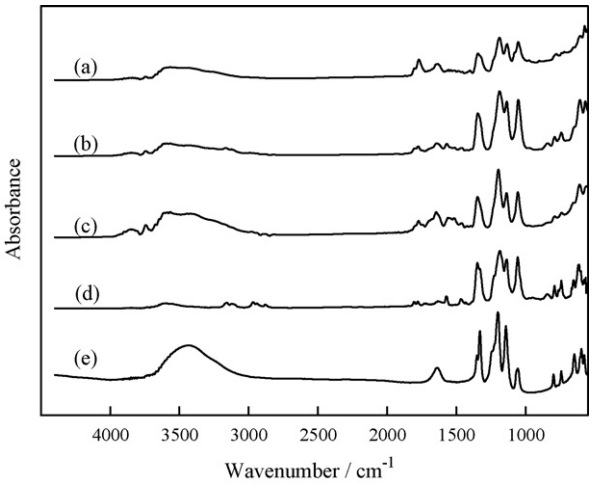

Fig. 5. FT-IR spectra of aluminum after CV in 1 M LiTFSI/EC + DMC (a); 1 M LiTFSI/EMI-TFSI (b); 1 M LiTFSI/PMI-TFSI (c); 1 M LiTFSI/BMI-TFSI (d), and of solid LiTFSI salt (e) as a reference.

presence of corrosion was influenced by the solvents used in electrolytes. In other words, the Al electrode was easily corroded in carbonate-based electrolyte, while it was rather stable in the RTILs. This behavior is in good agreement with the above CV results.

The anodic aluminum after the cyclic voltammetry was measured by FT-IR spectroscopy to identify the surface passive film which may possibly understand the complicated mechanism of corrosion and passivation in different electrolytes. The FT-IR spectrum of solid LiTFSI salt (Fig. 5(e)) was used as a reference. Peaks at 1329, 1200, 1141 and 1054 cm^{-1} assigned to $\upsilon_a(SO_2)$, $\upsilon_s(CF_3)$, $\upsilon_a(CF_3)$ and $\upsilon_s(SO_2)$, respectively, which characters the functional groups of bis[(trifluoromethyl)sulfonyl]amide ($TFSI^-$, $N(SO_2CF_3)_2^-$). In addition, the presence of $\delta(H_2O)$ band at 1638 cm^{-1} and broad $\nu(H_2O)$ bands around 3400 cm^{-1} trace the existence of water in lithium salt. Fig. 5(a) shows the FT-IR spectra of aluminum surface after the cyclic voltammetry in LiTFSI/EC + DMC solution. By referring to the spectra of LiTFSI salt, several peaks around 1344, 1188, 1136 and 1052 cm^{-1} were assigned to $\upsilon_a(SO_2)$, $\upsilon_s(CF_3)$, $\upsilon_a(CF_3)$ and $\upsilon_s(SO_2)$, respectively, coming from bis[(trifluoromethyl)sulfonyl] amide ($TFSI^-$, $N(SO_2CF_3)_2^-$) [26,27]. This spectral analysis indicated that some corrosion products compounded of $TFSI^-$ still existed on the aluminum surface around the pitting hole even the occurrence of aluminum corrosion in EC + DMC solution. Fig. 5(b)–(d) showed the FT-IR spectra of aluminum surface after the cyclic voltammetry in LiTFSI solutions with BMI-TFSI, PMI-TFSI and EMI-TFSI, respectively. Similarly, peaks at about 1346, 1186, 1136, 1056 cm^{-1} also assigned to $–SO_2$ and $–CF_3$ groups of $TFSI^-$. A broad band at 3300 cm^{-1} was ascribed to $\nu(H_2O)$ which may come from the trace of water in the RTILs except for tiny altitude spectra of Fig. 5(d) because the aluminum surface contained less amount of water after the anodic polarization in BMI-TFSI electrolyte. The observations of the FT-IR spectra showed that a functional group $TFSI^-$ existed on the aluminum surface after the cyclic voltammetry in LiTFSI solutions. Fig. 6

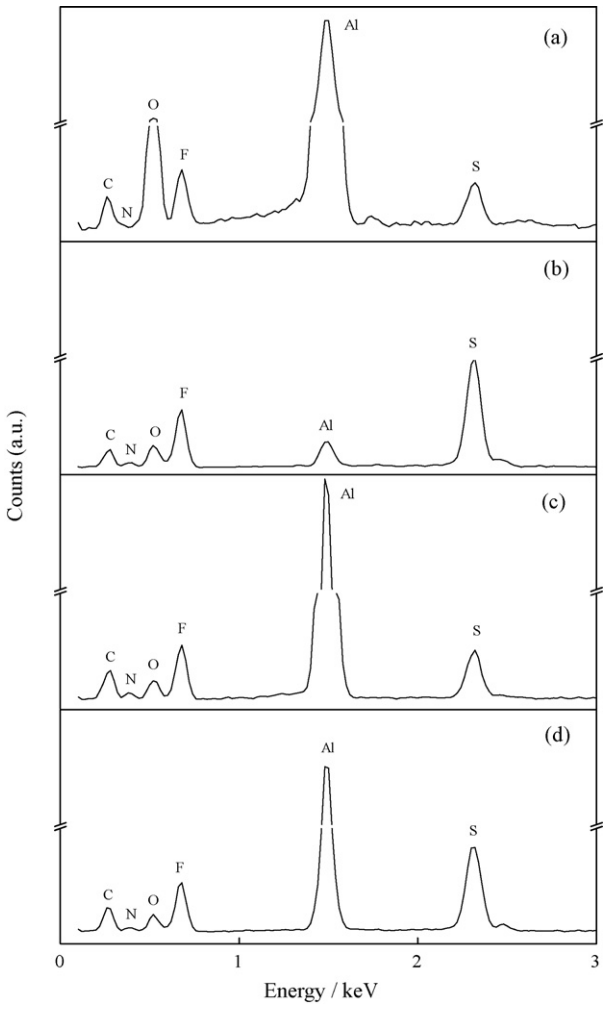

Fig. 6. EDX spectra of aluminum after CVs in LiTFSI/EC + DMC (a); 1 M LiTFSI/EMI-TFSI (b); 1 M LiTFSI/PMI-TFSI (c); 1 M LiTFSI/BMI-TFSI (d).

showed the EDX spectra of anodic aluminum foil in EC + DMC, EMI-TFSI, PMI-TFSI and BMI-TFSI containing LiTFSI. The elements of C, N, O, F and S were detected on the anodic aluminum foil in the above four electrolytes which were ascribed to the functional groups of $TFSI^-$. At the same time, larger amount of Al was also observed on the anodic Al foil surface except partly aluminum probably came from the substrate material, which indicated the presence of Al-TFSI precipitates over the surface film. In addition, a very larger amount of O with Al was observed on the Al foil surface after the anodic polarization in EC + DMC containing LiTFSI which indicated the presence of Al_2O_3 and also the oxidation compounds from the carbonate solvents except for Al-TFSI compounds around the aluminum pitting hole after the anodic polarization. It may come from the passive film covered on the pretreated aluminum surface. With previous reports [4], it was concluded that some corrosion products of Al-TFSI compounds were soluble in EC + DMC solvents, resulting in the occurrence of aluminum corrosion, while it did not dissolve in RTILs which firmly attached on the surface to become a protective film and inhibited further aluminum corrosion.

3.2. The anodic behavior of Al electrode in the BMI-TFSI with additives

Although RTILs has many attractive properties, they were still faced some practical problems when using as the electrolytes for lithium ion batteries. As some previous reports, it was observed that the capacity of $LiCoO_2$/Li coin cells with RTILs decreased rapidly and finally became impossible to charge the coin cell. Shiro et al. [28] and Fernicola et al. [20] reported that those RTILs lack electrochemical stability up to the reduction potential of lithium or lithiated carbon surface which led to the failure of charge/discharge process of lithium ion batteries. To solve the problems for practical use of the RTILs in lithium ion batteries, Takaya et al. [23] and Zheng et al. [24] reported that the addition of additives into the RTILs have improved the cycling performance of lithium ion batteries due to some amounts of additives in RTILs aiding the formation of solid electrolyte interface (SEI) on the negative electrode's active material surface which inhibited the further cathodic decomposition of electrolytes and protected the charged negative electrode. However, some sorts of additives may influence the passivation on aluminum surface, which resulting in the occurrence of aluminum corrosion. Therefore, the anodic behaviors of the Al current collector in the RTILs with the additives were necessary to be investigated. In this experiment, some kinds of additive, such as ethylene sulfite (ES), ethylene carbonate (EC), and vinyl carbonate (VC) which expected to prevent the decomposition and also improve the reversible lithium deposition/dissolution were chosen to add into BMI-TFSI as a representative to study the anodic polarization behavior of the Al foil in the RTILs with additives.

Fig. 7(a) showed cyclic voltammograms of the Al foil electrode in BMI-TFSI electrolytes with 10 wt.% ES. An anodic current increased abruptly at about 4.6 V during first cycle, and started to increase at 4.3 V from second cycle, reaching the maximum at 4.8 V during the potential sweep to cathodic direction though the maximum current then decreased by the following cycles. This type of voltammetric responses character that a less effective passive film formed on the Al surface was prone to the breakdown of the passive film and the dissolution of Al electrode during the anodic sweep. Whereas the anodic currents of aluminum in BMI-TFSI with 10 wt.% EC and 10 wt.% VC in Fig. 7(b) and (c) were much smaller than those observed in BMI-TFSI with the additive of 10 wt.% ES, the anodic current started to increase at about 3.5 V and decreased rapidly during the backward scan through the maximum at 5.5 V. During the next cycle, the anodic current increased higher than 5.0 V and the magnitude of the current smaller than that in the first cycle, which indicated that an effective passive film had formed on Al electrode during the first scan in the BMI-TFSI electrolytes. The voltammetric responses of Al electrode in the RTILs with 10 wt.% EC and 10 wt.% VC were similar to that in the RTILs with no additive, which implied that some amounts of EC or VC into the RTILs did not obviously influence the surface passivation of Al electrode. However, the smaller current density of Al current collector during the cyclic voltammetry measurement in LiTFSI/BMI-TFSI with 10 wt.% VC compared with that of the same electrolytes with 10 wt.% EC indicated that VC is more favorable for the stability of Al current collector in RTILs.

3.3. The anodic behavior of Al electrode in BMI-TFSI at different temperature

Compared with the commercial organic electrolytes, RTILs exhibits wide liquid phase range to apply as the electrolytes in lithium ion batteries. In addition, the viscosity decreased

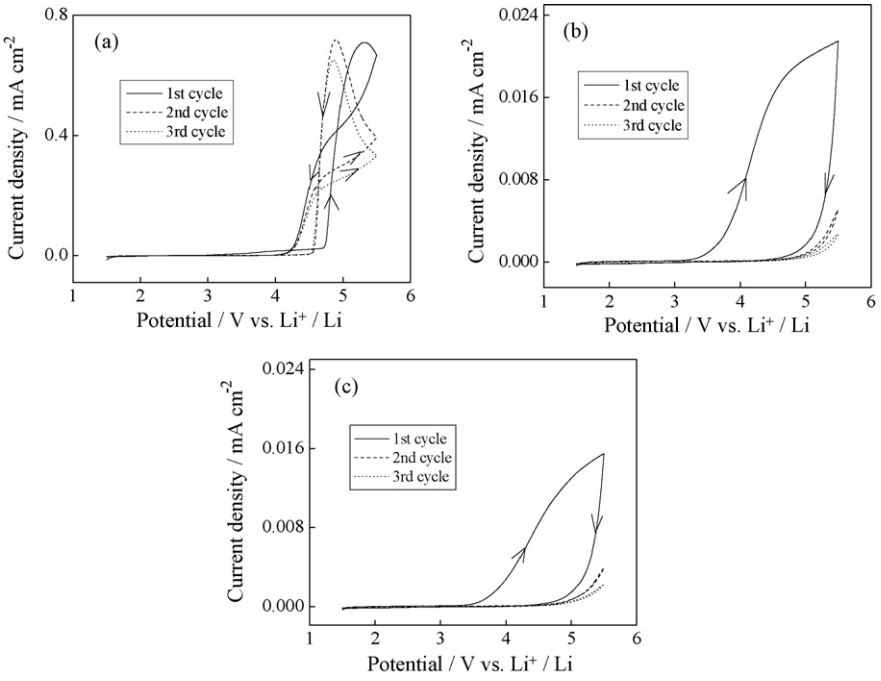

Fig. 7. Cyclic voltammograms for Al foil electrode in 1 M LiTFSI/BMI-TFSI with ES (a); EC (b); VC (c) (sweep rate: 10.0 mV s^{-1}).

and ion conductivities increased with increasing temperature which available for cycling performance of lithium ion batteries [29,30]. Hence, temperature was chose to study in an attempt to extend the application fields of lithium ion batteries, especially for the energy storage devices for aerospace outside of the earth and military uses.

Fig. 8 showed the cyclic voltammograms of Al foil electrode in 1 M LiTFSI/BMI-TFSI and its solution with 10% VC at 25, 40 and 60 °C. Whatever the existence of additives, it was found that the E_p of Al foil in the above two solutions shifted to more and more negative potential and the magnitude of current density increased with increasing temperature during the anodic polarization processes, the similar result was also reported in LiTFSI solutions with conventional organic solvents [10]. The results indicated that the increase of the oxidizability accelerated the reaction between aluminum and electrolytes at the elevated temperatures, which led to the E_p of Al shift to more negative potential. However, the current decreased rapidly and passive film still firmly formed on the aluminum surface after the first cycle and surpassed the further oxidation of aluminum current collector which can be benefit for the use of lithium ion batteries at high temperature.

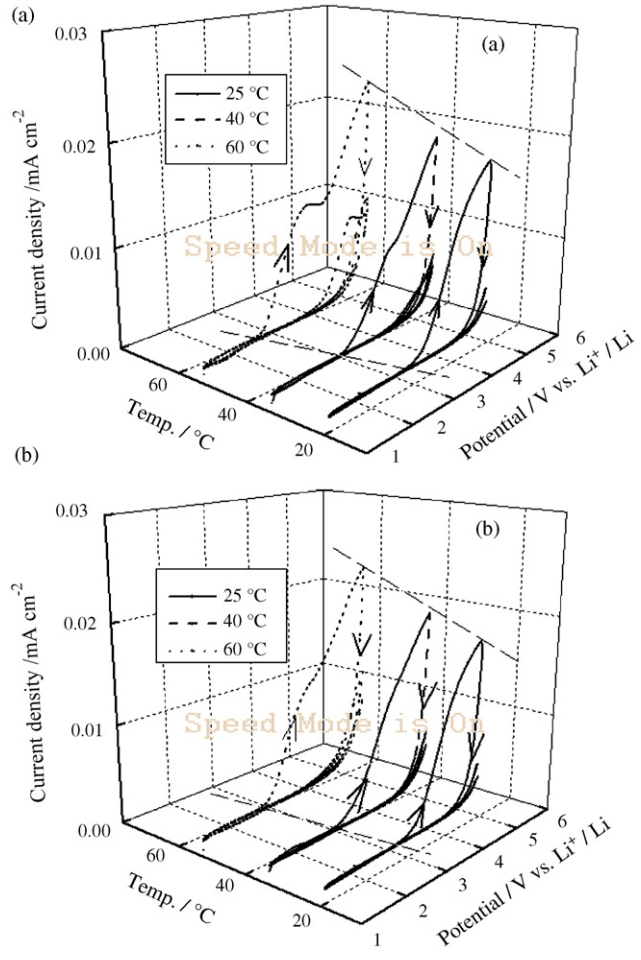

Fig. 8. Cyclic voltammograms for Al foil electrode in 1 M LiTFSI/BMI-TFSI (a); 1 M LiTFSI/BMI-TFSI with VC (b) at 25, 40 and 60 °C (sweep rate: 10.0 mV s^{-1}).

4. Conclusion

The anodic behaviors of Al in a series of 1-alkyl-3-methylimidazolium bis[(trifluoromethyl)sulfonyl] amide ionic liquids (EMI-TFSI, PMI-TFSI and BMI-TFSI) and EC + DMC both containing 1 M LiTFSI were investigated. It was found that aluminum corrosion occurred in EC + DMC solutions containing LiTFSI, while not found in RTILs electrolytes. The results indicated that EMI-TFSI, PMI-TFSI and BMI-TFSI could be used as candidates to inhabit the corrosion of aluminum current collector in the electrolytes containing LiTFSI, which led to the possibility for the use of LiTFSI salt with its interesting performance and higher safety in practical advanced lithium ion batteries. Moreover, it was found that BMI-TFSI is the most effective ionic liquid to inhibit the aluminum corrosion. At the same time, the addition of ES, EC and VC into the BMI-TFSI to inhibit the cathodic decomposition of electrolytes was also studied on the anodic behavior of aluminum. As a result, VC showed the best performance for stabilizing effect on aluminum current collector in the BMI-TFSI which may further enhanced the practical use of BMI-TFSI in lithium ion battery. In addition, the influence of temperature on the surface passive film was tested, only the E_p of Al foil shifted to more and more negative potential at the elevated temperature, a passive film still firmly formed on the aluminum surface which surpassed the further oxidation of aluminum current collector.

Acknowledgements

The authors thank the research center of analysis and measurement of Shanghai Jiao Tong University for his help in the SEM measurements. This work was sponsored by the National Key Project of China for Basic Research under Grant No.2006CB202600, the Scientific Research Foundation for the Returned Overseas Chinese Scholars supported by State Education Ministry, Shanghai Pujiang Program (No.05PJ14066) and the Open Foundation of State Key Laboratory of Physical Chemical of Solid Surfaces (No.200606).

References

[1] N. Terada, T. Yanagi, S. Arai, M. Yoshikawa, K. Ohta, N. Nakajima, A. Yanai, N. Arai, J. Power Sources 100 (2001) 80–92.
[2] A.K. Padhi, K.S. Nanjundasamy, J.B. Goodenough, J. Electrochem. Soc. 144 (4) (1997) 1188–1194.
[3] L.J. Krause, W. Lamanna, J. Summerfield, M. Engle, G. Korba, R. Loch, R. Atanasoski, J. Power Sources 68 (1997) 320–325.
[4] X. Wang, E. Yasukawa, S. Mori, Electrochim. Acta 45 (2000) 2677–2684.
[5] H. Yang, K. Kwon, T.M. Devine, J.W. Evans, J. Electrochem. Soc. 147 (12) (2000) 4399–4407.
[6] S.S. Zhang, T.R. Jow, J. Power Sources 109 (2002) 458–464.
[7] M. Morita, T. Shibata, N. Yoshimoto, M. Ishikawa, Electrochim. Acta 47 (2002) 2787–2793.
[8] M. Morita, T. Shibata, N. Yoshimoto, M. Ishikawa, J. Power Sources 119–121 (2003) 784–788.
[9] T. Kawamura, T. Tanaka, M. Egashira, I. Watanabe, S. Okada, J. Yamaki, Electrochem. Solid-State Lett. 8 (9) (2005) A459–A463.
[10] D. Di Censo, I. Exnar, M. Graetzel, Electrochem. Commun. 7 (2005) 1000–1006.
[11] W.K. Behl, E.J. Plichta, J. Power Sources 72 (1998) 132–135.

[12] T. Nakajima, M. Mori, V. Gupta, Y. Ohzawa, H. Iwata, Solid State Sci. 4 (2002) 1385–1394.
[13] S. Song, T.J. Richardson, G.V. Zhuang, T.M. Devine, J.W. Evans, Electrochim. Acta 49 (2004) 1483–1490.
[14] L.A. Blanchard, D. Hancu, E.J. Beckman, et al., Nature 399 (1999) 28–29.
[15] D.R. MacFarlane, J.H. Huang, M. Forsyth, Nature 402 (1999) 792–794.
[16] A. Noda, M. Watanabe, Electrochemistry 70 (2002) 140–144.
[17] M. Hirao, H. Sugimoto, H. Ohno, J. Electrochem. Soc. 147 (11) (2000) 4168–4172.
[18] Z.B. Zhou, H. Matsumoto, K. Tatsumi, Chem. Eur. J. 10 (2004) 6581–6591.
[19] A.B. McEwen, H.L. Ngo, K. LeCompte, J.L. Goldman, J. Electrochem. Soc. 146 (5) (1999) 1687–1695.
[20] A. Fernicola, B. Scrosati, H. Ohno, Ionics 12 (2006) 95–102.
[21] G. Béatrice, A. Michel, J. Power Sources 132 (2004) 206–208.
[22] J.L. Goldman, A.B. McEwen, Electrochem. Solid State Lett. 2 (101) (1999) 501–503.
[23] T. Sato, T. Maruo, S. Marukane, K. Takagi, J. Power Sources 138 (2004) 253–261.
[24] H. Zheng, K. Jiang, T. Abe, Z. Ogumi, Carbon 44 (2006) 203–210.
[25] P. Bonhôte, A. Dias, N. Papageorgiou, K. Kalyanasundaram, M. Grältzel, Inorg. Chem. 35 (1996) 1168–1178.
[26] G. Socrates, Infrared and Raman Characteristic Group Frequencies, Wiley, Chichester, 2007.
[27] R.A. Nyquist, R.O. Kagel, Handbook of Infrared and Raman spectra of Inorganic Compounds and Organic Salts, vol. 4, Academic Press, 1971.
[28] S. Shiro, K. Yo, M. Hajime, O. Yasutaka, M. Yuichi, U. Akira, T. Nobuyuki, W. Masayoshi, Electrochem. Solid-State Lett. 8 (11) (2005) A577–A578.
[29] B. Garcia, S. Lacallée, G. Perron, Ch. Michot, M. Armand, Electrochem. Acta 49 (2004) 4583–4588.
[30] M. Diaw, A. Chagnes, B. Carré, P. Willmann, D. Lemordant, J. Power Sources 146 (2005) 682–684.